RASĀYAN *J. Chem.*
Vol. 19 | No. 3 | 1816-1824 | July-September | 2026
ISSN: 0974-1496 | e-ISSN: 0976-0083 | CODEN: RJCABP
http://www.rasayanjournal.com
http://www.rasayanjournal.co.in

SYNTHESIS AND CHARACTERISATION OF 3-(CHLOROPHENYLHYDRAZO)-2,4-PENTANEDIONES AND THEIR METAL COMPLEXES WITH ENHANCED ANTIMICROBIAL ACTIVITY

Merin Sara and Muhammed Basheer Ummathur✉
PG and Research Department of Chemistry, KAHM Unity Women's College (Autonomous), Manjeri-676122(Kerala) India
✉Corresponding author: mbummathur@gmail.com

ABSTRACT

A series of 3-(chlorophenylhydrazo)-2,4-pentanediones along with their Cr(III), Mn(II), Fe(III), Co(II), Ni(II), Cu(II), and Zn(II) complexes were prepared and subsequently characterized through elemental composition, spectroscopic techniques (IR, UV–Vis, ^{1}H NMR, and mass), as well as magnetic and conductance measurements. Analytical results indicate an $[ML_3]$ stoichiometry for Cr(III) and Fe(III), while Mn(II) and Co(II) form complexes of the type $[M(L)_2(H_2O)_2]$, and Ni(II), Cu(II), and Zn(II) exhibit $[ML_2]$ composition. The ligands behave as monobasic bidentate species, coordinating via the deprotonated hydrazone nitrogen and the carbonyl oxygen involved in hydrogen bonding. This coordination mode results in octahedral structures for Cr(III), Mn(II), Fe(III), and Co(II), square-planar arrangements for Ni(II) and Cu(II), and a tetrahedral geometry for Zn(II). Antimicrobial evaluation against *Escherichia coli*, *Staphylococcus aureus*, and *Aspergillus niger* revealed enhanced activity upon metal coordination, with Mn(II), Ni(II), and Zn(II) complexes exhibiting the most significant effects. The observed variation in activity across the metal series highlights the critical role of metal ion identity, coordination geometry, and chelate stability in governing biological performance. This study advances medicinal inorganic chemistry by establishing clear structure–activity relationships in chloro-substituted hydrazone complexes and demonstrates that rational selection of metal ions and ligand frameworks can effectively tune antimicrobial properties. These results offer a basis for developing novel metal-containing antimicrobial agents aimed at tackling the increasing problem of antimicrobial resistance.

Keywords:3-(Chlorophenylhydrazo)-2,4-Pentanediones, Metal Complexes, Spectral Characterization, Coordination Geometry, Antimicrobial Activity.

RASĀYAN *J. Chem.*, Vol. 19, No.3, 2026

INTRODUCTION

The design and synthesis of metal complexes incorporating biologically active ligands continue to be an important area of research due to their wide-ranging applications in medicinal chemistry, catalysis, and materials science.[1] Among these, hydrazone-based ligands derived from 1,3-diketones have attracted considerable attention because of their versatile coordination behaviour and ability to form stable chelates with transition metal ions through enolic oxygen and azomethine nitrogen donor sites.[2,3] Structural modifications in such ligands, particularly through substitution on the aromatic ring, can significantly influence their electronic properties, coordination modes, and overall reactivity.[4] Transition metal complexes of hydrazone and β-diketone derivatives are well known for their diverse biological activities, including antibacterial, antifungal, and anticancer properties.[5,6] The presence of electron-withdrawing substituents such as chloro groups can enhance metal–ligand interactions, modulate lipophilicity, and influence biological activity by facilitating improved penetration through microbial cell membranes.[7,8] Furthermore, chelation is often associated with increased bioactivity due to reduced polarity of the metal ion and greater delocalisation of π-electrons, which enhances interaction with biological targets.[9] Recent studies continue to highlight the importance of such structural and electronic factors in determining the biological efficacy of coordination compounds.[5-9] Although some studies on phenylhydrazo-1,3-diketone metal complexes have been reported, the relationship between chloro substitution, metal ion identity, coordination geometry, and antimicrobial activity remains insufficiently explored.[10] A precise

understanding of these relationships is crucial for establishing structure–activity correlations and for guiding the rational development of more efficient metal-based antimicrobial agents. Therefore, the present study aims to address this gap through a comprehensive synthesis, characterization, and comparative biological evaluation of these complexes. In this context, the present work focuses on the synthesis of a series of 3-(chlorophenylhydrazo)-2,4-pentanediones along with their Cr(III), Mn(II), Fe(III), Co(II), Ni(II), Cu(II), and Zn(II) complexes, followed by comprehensive characterization and assessment of their antimicrobial activity. By systematically examining the coordination behaviour and biological activity of these compounds, the study seeks to provide insights into the role of metal ions and ligand frameworks in modulating antimicrobial efficacy. This study is consistent with Sustainable Development Goal-3 (Good Health and Well-being), as it emphasises the development of novel antimicrobial agents to combat infectious diseases and the rising threat of antimicrobial resistance. Transition metal complexes provide a versatile platform owing to their structural diversity and adjustable biological behaviour, and the present work advances medicinal inorganic chemistry toward the development of effective metal-based antimicrobial agents.

EXPERIMENTAL

Materials and Instrumentation

All chemicals used were of analytical grade and utilised without further purification. 2-, 3-, and 4-chloroanilines, acetylacetone, and metal acetates of Cr(III), Mn(II), Fe(III), Co(II), Ni(II), Cu(II), and Zn(II) were obtained from Merck and used as received. Solvents were purified using standard laboratory procedures prior to use. Elemental analyses (C, H, N) were carried out using a CHNS analyser (Unicube Elementar), and metal contents were determined by atomic absorption spectroscopy (PerkinElmer AAnalyst 400). Molar conductance measurements were performed in DMF (10^{-3}M) using a Schott Instruments conductivity meter. Magnetic susceptibilities were measured at room temperature using a Gouy balance (Sherwood Scientific, UK). IR spectra were recorded on an Agilent Cary FT-IR spectrometer (4000–400 cm^{-1}, KBr pellets). UV–Vis spectra were obtained in DMF using an Agilent Cary 5000 spectrophotometer. ^{1}H NMR spectra were recorded in DMSO-d_6 with TMS as an internal standard on a JEOL 500 MHz spectrometer. Mass spectra were acquired using a Waters Synapt XS high-resolution mass spectrometer coupled with an Acquity H-Class UPLC system. The antimicrobial activities were evaluated against *Escherichia coli*, *Staphylococcus aureus*, and *Aspergillus niger* using agar well diffusion, disk diffusion, and agar blot methods following reported procedures.[11,12]

Synthesis of 3-(Chlorophenylhydrazo)-2,4-pentanediones (HL^1–HL^3)

The ligands were synthesised by coupling diazotised chloroanilines with acetylacetone following reported procedures.[13,14] In a typical procedure, chloroaniline (0.075 mol) was subjected to diazotisation under standard conditions, and the freshly prepared diazonium solution was slowly introduced into a continuously stirred 50% (v/v) ethanol–water mixture containing acetylacetone (0.075 mol), maintained at 0–5 °C. Sodium acetate (~4 g) was then added to keep the pH in the range of 6–7. The reaction mixture was stirred until precipitation was complete. The product was filtered, washed with cold water, and recrystallised from hot methanol. The purified ligands were dried under vacuum and stored in a desiccator.

Synthesis of Metal Complexes

The metal complexes were obtained by interaction of the ligands with the respective metal acetates using suitable metal-to-ligand ratios [1:3 for Cr(III) and Fe(III), and 1:2 for Mn(II), Co(II), Ni(II), Cu(II), and Zn(II)], in agreement with the compositions presented in Table-1. The metal acetate was dissolved in 50 mL of 50% aqueous methanol, while the ligand was dissolved in ethanol with gentle heating (~60 °C). The metal solution was introduced gradually into the ligand solution with constant stirring, after which sodium acetate (~0.1 g) was added to promote deprotonation. The reaction mixture was refluxed for about 7 h. The precipitated complexes were then separated by filtration, rinsed with distilled water to eliminate residual starting materials, and finally dried under reduced pressure.

Antimicrobial Methods

For antibacterial studies, sterile nutrient agar plates were inoculated with bacterial suspensions (≈10^6 CFU/mL), and wells of approximately 6 mm diameter were prepared aseptically. Test solutions of the

compounds were introduced into the wells, and the plates were incubated at 37 °C for 24 h. Antibacterial activity was assessed by measuring the diameters of the inhibition zones (mm).[15] Antifungal activity was determined on potato dextrose agar plates, which were incubated at 28 °C for 48–72 h. The extent of antifungal activity was evaluated based on the clear zones formed around the test samples and expressed as percentage inhibition.[16] All experiments were performed in triplicate.

RESULTS AND DISCUSSION

Elemental analytical data for the ligands (Table-1) are consistent with the theoretical values, supporting the assigned molecular formulations (Fig.-1) and indicating a high degree of purity. The metal complexes were obtained as stable, non-hygroscopic solids. Analytical data (Table-1) correspond well with the proposed stoichiometries, namely $[ML_3]$ for Cr(III) and Fe(III), $[ML_2]$ for Ni(II), Cu(II), and Zn(II), and $[M(L)_2(H_2O)_2]$ for Mn(II) and Co(II). Molar conductance measurements in DMF (5–15 Ω^{-1} cm^2 mol^{-1}) suggest that the complexes behave as non-electrolytes, indicating coordination in the absence of counter ions, as illustrated in Fig.-2. These results are consistent with earlier reports on hydrazone-based coordination compounds, while the present study extends such investigations to chloro-substituted systems in a systematic manner. The inclusion of positional chloro substitution provides additional insight into substituent effects on coordination behaviour and stability, thereby addressing the limited comparative studies available in the literature.[10] Overall, this systematic comparison across multiple metal ions and substitution patterns offers clearer insight into structure–activity relationships.

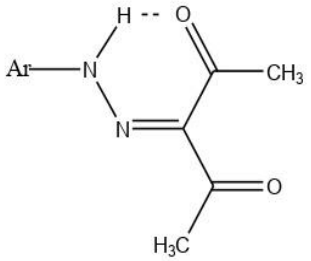

Fig.-1: Structure of 3-(chlorophenylhydrazo)pentane-2,4-diones

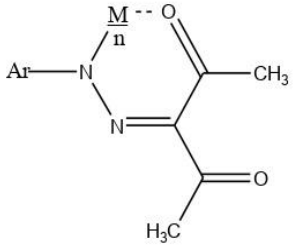

Fig.-2: Structure of metal complexes Ar = 2-chlorophenyl (HL^1); 3-chlorophenyl (HL^2); 4-chlorophenyl (HL^3) M = Cr^{3+}, Fe^{3+} (n = 3); Mn^{2+}, Co^{2+}, Ni^{2+}, Cu^{2+}, Zn^{2+} (n = 2) Mn(II) and Co(II) complexes also contain two coordinated water molecules

IR Spectra

All three ligands exhibit a characteristic broad absorption band in the 3190–3220 cm^{-1} region, attributable to hydrogen-bonded N–H stretching vibration. This indicates that the ligands predominantly adopt the keto–hydrazone tautomer, where the –NH moiety participates in strong intramolecular hydrogen bonding with a carbonyl oxygen atom, resulting in the stabilisation of a pseudo six-membered chelate ring. The carbonyl stretching region shows two distinct bands. The higher frequency band observed at 1663–1669 cm^{-1} is assigned to the non-hydrogen-bonded carbonyl group, while the lower frequency band appearing in the 1620–1633 cm^{-1} region is attributed to the carbonyl group involved in intramolecular hydrogen bonding with the –NH proton. This hydrogen bonding weakens the C=O bond, resulting in a noticeable shift to lower wavenumbers. The azomethine ν(C=N) stretching vibration is observed at 1580–1584 cm^{-1}, confirming the formation of the hydrazone linkage (Table-2).[17] Upon complexation, the disappearance of the broad N–H stretching band indicates deprotonation of the hydrazone nitrogen and subsequent involvement in coordination. Simultaneously, the hydrogen-bonded carbonyl band shifts to lower

frequencies in the range 1550–1580 cm^{-1}, suggesting further weakening of the C=O bond due to coordination of the adjacent donor atoms to the metal ion. The non-hydrogen-bonded carbonyl band remains largely unaffected, indicating that this carbonyl group does not participate in metal binding. New bands appearing in the 450–570 cm^{-1} region are assigned to ν(M–N) and ν(M–O) vibrations, providing direct evidence for metal–nitrogen and metal–oxygen bond formation (Table-3).[18,19] The presence of broad O–H stretching bands in Mn(II) and Co(II) complexes (3200–3500 cm^{-1}) confirms coordinated water molecules, supporting the proposed $[M(L)_2(H_2O)_2]$ formulation. These spectral changes, together with structural representations (Fig.-2), clearly establish the coordination mode of the ligands.

Table-1: Physical and Analytical Data of 3-(chlorophenylhydrazo)-2,4-pentanediones and their Metal Complexes

Compound	MP (°C)	Elemental Analysis (%): Calc (Found)			
		C	H	N	M
HL^1	130	55.60 (55.33)	4.21 (4.12)	11.80 (11.68)	–
HL^2	128	55.60 (55.47)	4.21 (4.17)	11.80 (11.70)	–
HL^3	131	55.60 (55.55)	4.21 (4.08)	11.80 (11.78)	–
$[CrL^1_3]$	287	51.91 (51.08)	3.93 (3.45)	11.00 (10.89)	6.81 (6.75)
$[CrL^2_3]$	285	51.91 (51.79)	3.93 (3.90)	11.00 (10.87)	6.81 (6.73)
$[CrL^3_3]$	280	51.91 (51.60)	3.93 (3.87)	11.00 (10.98)	6.81 (6.60)
$[Mn(L^1)_2(H_2O)_2]$	252	46.71 (46.58)	4.25 (4.18)	9.91 (9.80)	9.72 (9.56)
$[Mn(L^2)_2(H_2O)_2]$	249	46.71 (46.67)	4.25 (4.03)	9.91 (9.83)	9.72 (9.70)
$[Mn(L^3)_2(H_2O)_2]$	259	46.71 (46.20)	4.25 (4.15)	9.91 (10.10)	9.72 (10.06)
$[FeL^1_3]$	277	51.60 (51.53)	3.91 (3.82)	10.95 (10.63)	7.28 (7.23)
$[FeL^2_3]$	275	51.60 (51.47)	3.91 (3.67)	10.95 (10.73)	7.28 (7.14)
$[FeL^3_3]$	278	51.60 (51.47)	3.91 (3.72)	10.95 (10.33)	7.28 (7.21)
$[Co(L^1)_2(H_2O)_2]$	262	46.40 (46.34)	4.21 (4.13)	9.84 (9.78)	10.35 (10.33)
$[Co(L^2)_2(H_2O)_2]$	265	46.40 (46.33)	4.21 (4.18)	9.84 (9.77)	10.35 (10.30)
$[Co(L^{3v}(H_2O)_2]$	268	46.40 (46.37)	4.21 (4.11)	9.84 (9.78)	10.35 (10.26)
$[NiL^1_2]$	255	49.55 (49.50)	3.75 (3.67)	10.94 (10.87)	11.55 (11.48)
$[NiL^2_2]$	257	49.55 (49.47)	3.75 (3.72)	10.94 (10.78)	11.55 (11.38)
$[NiL^3_2]$	258	49.55 (49.43)	3.75 (3.63)	10.94 (10.77)	11.55 (11.45)
$[CuL^1_2]$	262	49.11 (49.08)	3.72 (3.69)	10.41 (10.34)	11.82 (11.79)
$[CuL^2_2]$	264	49.11 (49.07)	3.72 (3.58)	10.41 (10.36)	11.82 (11.67)
$[CuL^3_2]$	267	49.11 (49.08)	3.72 (3.63)	10.41 (10.39)	11.82 (11.77)
$[ZnL^1_2]$	225	48.90 (48.83)	3.71 (3.67)	10.41 (10.23)	12.12 (12.07)
$[ZnL^2_2]$	230	48.90 (48.86)	3.71 (3.63)	10.41 (10.39)	12.12 (12.10)
$[ZnL^3_2]$	233	48.90 (48.84)	3.71 (3.68)	10.41 (10.33)	12.12 (12.01)

Table-2: IR Spectral Bands (cm^{-1}) of 3-(chlorophenylhydrazo)-2,4-pentanediones

Ligand	ν(N–H)	Free ν(C=O)	H-bonded ν(C=O)	ν(C=N)
HL^1	3212 br	1669 s	1630 s	1584 s
HL^2	3200 br	1667 s	1633 s	1582 s
HL^3	3190 br	1663 s	1620 s	1580 s

^{1}H NMR Spectra

The ^{1}H NMR spectra of the ligands (Table-4) exhibit a characteristic broad singlet at δ 13.60–13.80 ppm, assigned to the hydrazone-NH proton involved in strong intramolecular hydrogen bonding with one of the carbonyl oxygen atoms.[20,21] This interaction stabilises the ligand framework through the formation of a pseudo-six-membered ring. Aromatic protons appear in the δ 7.37–7.70 ppm region, while the methyl protons of the acetylacetone moiety resonate as a singlet at δ 2.40–2.48 ppm, corresponding to six equivalent protons. In the Zn(II) complexes, the disappearance of the downfield –NH signal confirms deprotonation of the hydrazone nitrogen and its involvement in coordination to the metal ion. The disruption of intramolecular hydrogen bonding involving the carbonyl group further supports its participation in coordination through oxygen donation. The aromatic proton signals shift slightly downfield to δ 7.58–7.72 ppm due to decreased electron density upon metal binding. The methyl protons

appear as two closely spaced singlets in the δ 2.37–2.51 ppm region, reflecting reduced symmetry and a more rigid environment after chelation (Table-4). These spectral changes clearly indicate coordination through the deprotonated hydrazone nitrogen and the oxygen atom of the hydrogen-bonded carbonyl group, leading to stable bidentate chelate formation around the metal ion.[22]

Table-3: Spectral (IR, UV–Vis) and Magnetic Moment Data of the Metal Complexes of 3-(chlorophenylhydrazo)-2,4-pentanediones

Complex	ν(C=O) Chelated (cm^{-1})	ν(M–N) (cm^{-1})	ν(M–O) (cm^{-1})	UV (nm) π→π*, n→π*	LMCT (nm)	d–d Transitions (nm)	Magnetic Moment (B.M.)
$[CrL^1_3]$	1556	570	457	270, 380	480-540	530, 610	3.85
$[CrL^2_3]$	1550	567	448	275, 376	485-540	525, 615	3.87
$[CrL^3_3]$	1553	500	443	270, 383	490-545	535, 620	3.89
$[Mn(L^1)_2(H_2O)_2]$	1545	530	453	270, 353	453-460	520,580	5.88
$[Mn(L^2)_2(H_2O)_2]$	1553	534	456	270, 355	455-460	525, 575	5.90
$[Mn(L^3)_2(H_2O)_2]$	1565	543	460	272, 360	457-460	530, 570	5.95
$[FeL^1_3]$	1559	530	449	280, 375	440-480	535, 600	5.90
$[FeL^2_3]$	1563	534	455	275, 355	442-460	530, 610	5.91
$[FeL^3_3]$	1568	540	476	285, 362	445-460	537, 615	5.92
$[Co(L^1)_2(H_2O)_2]$	1564	503	468	275, 360	468-476	520, 570	4.78
$[Co(L^2)_2(H_2O)_2]$	1569	509	471	273, 365	468-475	509, 565	4.79
$[Co(L^3)_2(H_2O)_2]$	1575	520	476	280, 368	469-476	525, 574	4.80
$[NiL^1_2]$	1568	507	446	270, 375	438-446	–	-
$[NiL^2_2]$	1574	515	443	273, 377	440-446	–	-
$[NiL^3_2]$	1578	527	438	275, 380	442-446	–	-
$[CuL^1_2]$	1551	509	470	271, 365	470-484	615, 680	1.91
$[CuL^2_2]$	1558	513	479	274, 370	472-484	617, 675	1.92
$[CuL^3_2]$	1524	517	484	280, 380	474-484	620, 680	1.93
$[ZnL^1_2]$	1558	495	–	272, 363	272-370	–	-
$[ZnL^2v]$	1567	505	–	275, 365	273-370	–	-
$[ZnL^3_2]$	1573	513	–	278, 370	275-370	–	-

Table-4: ^1H NMR Spectral Data of 3-(chlorophenylhydrazo)-2,4-pentanediones and their Zn(II) Complexes

Compound	NH (δ, ppm)	Aromatic (δ, ppm)	CH_3 (δ, ppm)
HL^1	13.80 (br s)	7.37–7.57 (4H)	2.48 (6H)
HL^2	13.72 (br s)	7.45–7.70 (4H)	2.43 (6H)
HL^3	13.60 (br s)	7.47–7.65 (4H)	2.40 (6H)
$[ZnL^1_2]$	–	7.58–7.60 (8H)	2.45–2.51 (12H)
$[ZnL^2_2]$	–	7.69–7.72 (8H)	2.42–2.44 (12H)
$[ZnL^3_2]$	–	7.63–7.66 (8H)	2.37–2.41 (12H)

Mass Spectra

The mass spectra of the ligands (Table-5) display molecular ion peaks at *m/z* 237–239, corresponding to the characteristic isotopic pattern of chlorine ($^{35}Cl/^{37}Cl$), thereby confirming the presence of a single chloro substituent in each ligand molecule.[23] The M and M+2 peaks confirm the natural isotopic pattern of chlorine, while the fragmentation pattern supports the proposed structure through cleavage of the acetylacetone moiety and formation of stable hydrazone fragments. In the Cu(II) complexes, molecular ion peaks observed in the range *m/z* 536–541 (Table-5) confirm the formation of metal–ligand complexes. The isotopic pattern in this region reflects the presence of copper isotopes ($^{63}Cu/^{65}Cu$), providing additional confirmation of metal incorporation.[24] The appearance of these peaks, along with their corresponding fragment ions, is in good agreement with the proposed $[CuL_2]$ stoichiometry as in Fig.-2.

Table-5: Mass Spectral Data of 3-(chlorophenylhydrazo)-2,4-pentanediones and Metal Complexes

Compound	Important mass spectral peaks (m/z)
HL^1	237, 238, 239,222, 209, 194

HL^2	237, 238, 239, 222, 209, 194
HL^3	237, 238, 239, 222, 209, 194
$[CuL^1{}_2]$	536, 538, 540, 501, 480, 455, 430, 403
$[CuL^2{}_2]$	536, 538, 540, 501, 480, 455, 430, 403
$[CuL^3{}_2]$	536, 538, 540, 501, 480, 455, 430, 403

Electronic Spectra and Geometry

The UV–Vis spectra of the ligands in ethanol display intense π→π* transitions at ~260 nm and weaker n→π* transitions around ~360 nm, characteristic of the conjugated hydrazone system.[25] These transitions reflect the extended delocalisation of π-electrons over the phenyl ring, azomethine linkage, and carbonyl group. Upon coordination, these bands exhibit slight bathochromic shifts, indicating stabilisation of the π* orbitals due to metal–ligand interaction.[26] The Cr(III) complexes exhibit ligand-to-metal charge transfer (LMCT) bands in the 480–545 nm region along with weak d–d transitions at 525–620 nm. The observed magnetic moments (3.85–3.89 B.M.) correspond to three unpaired electrons, confirming a high-spin d^3 configuration in an octahedral environment.[27] These spectral and magnetic features are consistent with $[CrL_3]$ octahedral geometry. Mn(II) complexes show LMCT bands at 453–460 nm and weak d–d transitions in the 520–580 nm region. The magnetic moment values (5.88–5.95 B.M.) are characteristic of high-spin d^5 systems with five unpaired electrons, supporting octahedral geometry. The coordination sphere is completed by two water molecules, leading to the formulation $[Mn(L)_2(H_2O)_2]$. The presence of both ligand field transitions and coordinated solvent molecules highlights the flexibility of Mn(II) in accommodating six-coordinate environments.[28] Fe(III) complexes display LMCT bands at 440–460 nm and d–d transitions at 530–615 nm. Their magnetic moments (5.90–5.92 B.M.) confirm the presence of five unpaired electrons in a high-spin octahedral configuration.[29] These data support the formation of neutral $[FeL_3]$ complexes with octahedral geometry. Co(II) complexes exhibit LMCT bands at 468–476 nm and d–d transitions in the 509–574 nm region. The magnetic moment values (4.78–4.80 B.M.) are consistent with high-spin octahedral Co(II). The presence of coordinated water molecules in $[Co(L)_2(H_2O)_2]$ contributes to the stabilization of the octahedral geometry, with slight distortions indicated by weak shoulders in the visible region.[28] Ni(II) complexes display LMCT bands at 438–446 nm, while d–d transitions are not prominently observed in the UV–Vis region, as expected for square-planar d^8 systems. These complexes are diamagnetic, confirming the absence of unpaired electrons and supporting a square-planar geometry.[28] The spectral behaviour is consistent with strong ligand field stabilization in a planar environment. Cu(II) complexes show LMCT bands at 470–484 nm and broad d–d transitions in the 615–680 nm region. The magnetic moments (1.91–1.93 B.M.) correspond to a single unpaired electron, characteristic of d^9 systems. The broadness of the d–d bands is attributed to Jahn–Teller distortion, supporting a square-planar geometry.[28] Zn(II) complexes, with a d^{10} electronic configuration, show only charge transfer bands in the 272–370 nm region. These complexes are diamagnetic and adopt a tetrahedral geometry. Overall, the combined electronic spectral data and magnetic moment values (Table-3) provide strong evidence for the proposed geometries. The systematic variation in geometry across the metal ions highlights the role of electronic configuration and ligand field effects in determining coordination behaviour.

Antimicrobial Activity and Significance

The antimicrobial activity data (Table-6) indicate that both the ligands and their metal complexes exhibit appreciable biological activity against *Escherichia coli*, *Staphylococcus aureus*, and *Aspergillus niger*. The free ligands show moderate to good antibacterial activity, with inhibition zones in the range of 10–18 mm for *Escherichia coli* and 9–30 mm for *Staphylococcus aureus*, along with antifungal activity of 70–75%. Notably, HL^2 exhibits comparatively higher activity against *Staphylococcus aureus*, indicating that ligand structure plays a significant role in biological performance. This behaviour may be attributed to the presence of hydrazone and carbonyl functional groups, which facilitate interactions with microbial cell components.

Upon coordination, an enhancement in antimicrobial activity is observed in several cases, although the effect is not uniform across all complexes. The metal complexes exhibit inhibition zones in the range of

8–28 mm against *Escherichia coli* and 6–42 mm against *Staphylococcus aureus*, while antifungal activity varies from 0 to 100% depending on the metal ion and ligand. This behaviour can be explained on the basis of chelation theory, where coordination reduces the polarity of the metal ion through partial sharing of positive charge with donor atoms and increases lipophilicity, thereby facilitating membrane permeability.[30,31] Among the complexes, certain Mn(II), Ni(II), and Zn(II) derivatives exhibit comparatively higher antimicrobial activity. Notably, the Ni(II) complex $[NiL^2_2]$ shows the highest activity against *Staphylococcus aureus*, followed by the Mn(II) complex $[Mn(L^3)_2(H_2O)_2]$ and the Zn(II) complex $[ZnL^3_2]$, with the highest inhibition zone reaching 42 mm, higher than that of ampicillin under the present experimental conditions. In contrast, some complexes display only minimal inhibition, indicating limited antibacterial effectiveness in certain coordination environments. In terms of antifungal activity, Mn(II), Zn(II), and Co(II) complexes exhibit complete inhibition (100%) against *Aspergillus niger*, whereas Ni(II) complexes show ligand-dependent behaviour. In contrast, Cr(III) and Fe(III) complexes exhibit relatively lower antibacterial activity and no antifungal effect, suggesting that higher oxidation state metals with more inert coordination environments may limit biological interactions. Cu(II) complexes display moderate antibacterial and antifungal activity, while Co(II) complexes, though less active against bacteria, demonstrate excellent antifungal efficiency. The variation in antimicrobial activity across the series highlights the significant influence of the metal ion, coordination environment, and chelate stability on biological efficacy. Complexes with more labile coordination sites and favourable lipophilicity tend to exhibit enhanced activity, whereas more inert systems show comparatively reduced performance. These observations provide useful insights into structure–activity relationships and suggest that appropriate selection of metal ions and ligand frameworks can effectively modulate biological properties. The enhanced activity of certain complexes underscores their potential for further pharmacological investigation. These findings further support Sustainable Development Goal 3 (Good Health and Well-being), as they demonstrate the potential of metal-based compounds in addressing microbial infections and antimicrobial resistance. The structure–activity insights further support the rational design of more effective antimicrobial agents.

Table-6: Antibacterial and Antifungal Activity of 3-(chlorophenylhydrazo)-2,4-pentanediones and their Metal Complexes

Compound	*Inhibition Zone (mm)*				*Aspergillus niger* (%)
	Escherichia coli		*Staphylococcus aureus*		
	(50 µg/mL)	100 µg/mL	50 µg/mL	100 µg/mL	
HL^1	10	12	10	9	70
HL^2	12	13	25	30	70
HL3	15	18	15	18	75
$[CrL^1_3]$	11	13	10	11	0
$[CrL^2_3]$	9	11	10	14	0
$[CrL^3_3]$	8	12	8	8	0
$[Mn(L^1)_2(H_2O)_2]$	10	15	8	8	100
$[Mn(L^2)_2(H_2O)_2]$	21	28	8	11	100
$[Mn(L^3)_2(H_2O)_2]$	14	17	30	37	100
$[FeL^1_3]$	10	13	13	17	0
$[FeL^2_3]$	11	15	11	14	0
$[FeL^3_3]$	13	17	13	17	0
$[Co(L^1)_2(H_2O)_2]$	8	12	8	8	100
$[Co(L^2)_2(H_2O)_2]$	10	14	10	15	100
$[Co(L^3)_2(H_2O)_2]$	14	19	8	12	100
$[NiL^1_2]$	15	19	8	11	70
$[NiL^2_2]$	15	18	35	42	70
$[NiL^3_2]$	16	19	6	6	100
$[CuL^1_2]$	10	14	7	11	70
$[CuL^2_2]$	13	16	11	14	70
$[CuL^3_2]$	15	18	15	18	70

$[ZnL^1_2]$	15	19	12	16	100
$[ZnL^2_2]$	20	24	14	17	100
$[ZnL^3_2]$	18	21	30	35	100
Ampicillin	15	20	25	33	-
Nystatin	-	-	-	-	100

CONCUSION

A series of chloro-substituted phenylhydrazo-1,3-diketones and their Cr(III), Mn(II), Fe(III), Co(II), Ni(II), Cu(II), and Zn(II) complexes were synthesised and characterised. Analytical, spectral, and magnetic studies established that the ligands act as monobasic bidentate donors coordinating through the deprotonated hydrazone nitrogen and the oxygen atom of the hydrogen-bonded carbonyl group, forming $[ML_3]$ (Cr(III), Fe(III)), $[M(L)_2(H_2O)_2]$ (Mn(II), Co(II)), and $[ML_2]$ (Ni(II), Cu(II), Zn(II)) complexes. The proposed geometries-octahedral for Cr(III), Mn(II), Fe(III), and Co(II); square-planar for Ni(II) and Cu(II); and tetrahedral for Zn(II)-were well supported by electronic spectral data and magnetic moment values. Biological evaluation showed enhanced antimicrobial activity for the metal complexes compared to the free ligands, with Mn(II), Ni(II), and Zn(II) complexes being the most active. These results demonstrate that metal ion selection and coordination environment play a key role in determining biological efficacy and provide useful guidance for the design of metal-based antimicrobial agents. From an application perspective, these findings highlight the potential of rational ligand design and metal ion selection in developing effective metal-based antimicrobial agents. This work aligns with Sustainable Development Goal 3 (Good Health and Well-being) by aiding efforts to address microbial infections and the increasing issue of antimicrobial resistance. Further investigations on the mechanism of action, toxicity, and in vivo evaluation are recommended to advance these complexes toward practical applications.

ACKNOWLEDGMENTS

The authors gratefully acknowledge the National Institute of Technology (NIT), Calicut; the Central Sophisticated Instrumentation Facility (CSIF), University of Calicut; and the Inter University Instrumentation Centre (IUIC), Mahatma Gandhi University, for providing spectral facilities.

CONFLICT OF INTERESTS

Both authors declare that there is no conflict of interest in connection with the publication of this article.

AUTHOR CONTRIBUTIONS

The present work is related to *SDG-3: Good Health and Well-being*. All the authors contributed significantly to this manuscript, participated in reviewing/editing and approved the final draft for publication. The research profile of the authors can be verified from their ORCID ids, given below:

Merin Sara http://orcid.org/0009-0008-1129-6501
Muhammed Basheer Ummathur http://orcid.org/0000-0002-9894-7176

Cite this article as: M. Sara and M. B. Ummathur, *Rasayan J. Chem.*, 19(3), 1816-1824(2026), https://doi.org/10.31788/RJC.2026.1939721

REFERENCES

1. S. Adhikari, P. Nath, A. Das, A. Datta, N. Baildya, A. K. Duttaroy and S. Pathak, *Biomedicine & Pharmacotherapy*, **171**, 116211(2024), https://doi.org/10.1016/j.biopha.2024.116211
2. K. T. Mahmudov, *Coordination Chemistry Reviews*, **265**, 1(2014), https://doi.org/10.1016/j.ccr.2014.01.002
3. M. N. Kopylovich, K. T. Mahmudov, M. F. C. Guedes da Silva, P. J. Figiel, Y. Y. Karabach, M. L. Kuznetsov, K. V. Luzyanin and A. J. L. Pombeiro, *Inorganic Chemistry*, **50**, 918(2011), https://doi.org/10.1021/ic101516k

4. Z. Moussa, M. Al-Mamary, S. Al-Juhani and S. A. Ahmed, *Heliyon*, **6**, e05019(2020), https://doi.org/10.1016/j.heliyon.2020.e05019
5. I. Czyżewska, L. Mazur and Ł. Popiołek, *Chemical Biology & Drug Design,* **104**, e14590(2024), https://doi.org/10.1111/cbdd.14590
6. A. F. Shoair, A. A. El-Bindary, N. A. El-Ghamaz and G. N. Rezk, *Journal of Molecular Liquids*, **269**, 619(2018), https://doi.org/10.1016/j.molliq.2018.08.075
7. W.-Y. Fang, L. Ravindar, K. P. Rakesh, H. M. Manukumar, C. S. Shantharam, N. S. Alharbi and H. L. Qin, *European Journal of Medicinal Chemistry*, **173**, 117(2019), https://doi.org/10.1016/j.ejmech.2019.03.063
8. R. Liu, J. Cui, T. Ding, Y. Liu and H. Liang, *Molecules*, **27**, 8393(2022), https://doi.org/10.3390/molecules27238393
9. B. Sharma, S. Shukla, R. Rattan, M. Fatima, M. Goel, M. Bhat, S. Dutta, R. K. Ranjan and M. Sharma, *International Journal of Biomaterials*, **2022**, 6819080(2022), https://doi.org/10.1155/2022/6819080
10. P. T. Malini, M. B. Ummathur, D. K. Babu and K. Krishnankutty, *Rasayan Journal of Chemistry*, **14**, 2111(2021), http://doi.org/10.31788/RJC.2021.1436292
11. I. V. Mañozca-Dosman, A. Aragón-Muriel and D. Polo-Cerón, *Scientia Pharmaceutica*, **93,** 22(2025), https://doi.org/10.3390/scipharm93020022
12. M. Claudel, J. V. Schwarte and K. M. Fromm, *Chemistry*, **2**, 849(2020), https://doi.org/10.3390/chemistry2040056
13. K. H. Saunders and R. L. M. Allen, *Aromatic Diazo Compounds*, 3rd ed., Hodder Arnold, New Delhi, 1985.
14. C. J. Patil, D. S. Talele, S. P. Talele, P. R. Pohekar and A. S. Patil, *International Journal of Pharmaceutical Sciences Review and Research*, **70**, 75(2021), http://dx.doi.org/10.47583/ijpsrr.2021.v70i02.011
15. T. Rakshit, A. Haldar, S. Jana, S. Raha, R. Saha and D. Mandal, *Results in Chemistry*, **6**, 101224(2023), https://doi.org/10.1016/j.rechem.2023.101224
16. M. C. Rathod, V. J. Godhani and D. A. Dhale, *World Journal of Pharmacy and Pharmaceutical Sciences*, **4**, 1323(2015).
17. L. J. Bellamy, *The Infra-red Spectra of Complex Molecules*, 3rd ed., Chapman & Hall, London, 1975.
18. T. Maldonado, E. Flores, L. Llanos, D. Aravena, A. Vega, F. Godoy, A. Aspée, N. Arancibia-Miranda, G. Ferraudi and A. Gómez, *Dyes and Pigments*, **197**, 109953(2022), https://doi.org/10.1016/j.dyepig.2021.109953
19. K. Nakamoto, *Infrared and Raman Spectra of Inorganic and Coordination Compounds*, 6th ed., Wiley, Hoboken, 2009.
20. A. Lyčka, *Dyes and Pigments*, **43**, 27(1999), https://doi.org/10.1016/S0143-7208(99)00032-7
21. O. O. Olakojo, E. Beitz, U. Girreser, A. O. Adegoke and S. O. Idowu, *Journal of Chemical Sciences*, **137**, 83(2025), https://doi.org/10.1007/s12039-025-02425-3
22. V. Raman, S. Muthuraj, S. Ravichandran and A. Kulandaisamy, *Journal of Chemical Sciences*, **115**, 161(2003), https://doi.org/10.1007/BF02704255
23. D. K. Holdsworth, *Journal of Chemical Education*, **59**, 780(1982), https://doi.org/10.1021/ed059p780
24. S. T. Hamdi, *Monatshefte für Chemie-Chemical Monthly*, **123**, 1081(1992), https://doi.org/10.1007/BF00808270
25. E. Wagner-Wysiecka, N. Łukasik, J. F. Biernat and E. Luboch, *Journal of Inclusion Phenomena and Macrocyclic Chemistry*, **90**, 189(2018), https://doi.org/10.1007/s10847-017-0779-4
26. N. A. Bhise, S. A. Al-horaibi, S. T. Gaikwad and A. S. Rajbhoj, *Rasayan Journal of Chemistry*, **12**, 101(2019), http://dx.doi.org/10.31788/RJC.2019.1214045
27. S. F. A. Kettle, *Electronic Spectra of Transition Metal Complexes*, in *Physical Inorganic Chemistry*, Springer, Berlin, 1996.
28. S. Chandra and R. Kumar, *Spectrochimica Acta Part A: Molecular and Biomolecular Spectroscopy*, **61**, 437(2005), https://doi.org/10.1016/j.saa.2004.04.018
29. A. T. Pilipenko, L. I. Savranskii and N. A. D'yachenko, *Journal of Applied Spectroscopy*, **19**, 882(1973), https://doi.org/10.1007/BF00606853
30. R.S. Joseyphus and M.S. Nair, *Mycobiology*, **36**, 93(2008), https://doi.org/10.4489/MYCO.2008.36.2.093
31. Q.-u.-Ain, A. Abid, M. Lateef, N. Rafiq, S. Eijaz, S. Tauseef, *Biomedicine & Pharmacotherapy*, **146**, 112561(2022), https://doi.org/10.1016/j.biopha.2021.112561 [RJC-9721/2026]